Journal of Global Antimicrobial Resistance 17 (2019) 263–275

Contents lists available at ScienceDirect

Journal of Global Antimicrobial Resistance

journal homepage: www.elsevier.com/locate/jgar

Magnesium deprivation affects cellular circuitry involved in drug resistance and virulence in *Candida albicans*

Sandeep Hans, Zeeshan Fatima*, Saif Hameed*

Amity Institute of Biotechnology, Amity University Haryana, Gurugram (Manesar), Haryana 122413, India

ARTICLE INFO

Article history:
Received 21 July 2018
Received in revised form 28 November 2018
Accepted 7 January 2019
Available online 16 January 2019

Keywords:
Candida
Magnesium
Cell membrane
Morphogenesis
Biofilm
Glyoxylate cycle

ABSTRACT

Objectives: Candida albicans has to struggle for the limited micronutrients present in the hostile host niche, including magnesium (Mg). The aim of this study was to examine the effect of Mg deprivation on drug resistance mechanisms and virulence traits of *C. albicans*.
Methods: The drug susceptibility of *C. albicans* strain SC5314 was determined by broth microdilution and spot assay. Efflux pump activity was measured using the substrate rhodamine 6G. Membrane intactness was studied by propidium iodide influx, and ergosterol levels were determined by the alcoholic KOH method. Metabolic flexibility was examined by studying the activity of glyoxylate cycle enzymes. Virulence factors were assessed by yeast-to-hyphae transition, biofilm formation and cell adherence. An in vivo study was also performed in a *Caenorhabditis elegans* infection model.
Results: Mg chelation leads to potentiation of membrane-targeting antifungals. The role of Mg on membrane homeostasis was explored and significant differences in ergosterol levels were found. Interestingly, it was also observed that Mg deprivation impedes the metabolic flexibility of *C. albicans* SC5314 by inhibiting glyoxylate cycle enzymes. Furthermore, Mg deprivation inhibited potential virulence traits, including morphological transition, biofilm formation and buccal epithelial cell adherence. All of the disrupted gene targets were validated by reverse transcription PCR. Lastly, enhanced survival of *C. elegans* infected with *C. albicans* SC5314 under Mg deprivation was observed.
Conclusion: In view of the restricted growth of *C. albicans* in a Mg-deficient environment, approaches could be utilised to boost the effectiveness of existing antifungals thereby improving the management of fungal infections.

1. Introduction

Candida albicans is an opportunistic human fungal pathogen causing both mucosal and invasive infections in immunocompromised patients [1]. The advent of multidrug resistance has led to a reduction in the effectiveness of antifungal drugs, commanding an urgent need to look for novel treatment strategies. One feature that pathogenic micro-organisms, including *C. albicans*, must surmount to establish successful infection is micronutrient stress, since micronutrients are not freely available in the host. Micronutrients are required for diverse enzymatic and structural roles. The host deliberately withholds metals such as Fe, Zn, Mn and Mg from invading microbes as a defence strategy known as nutritional immunity [2]. Thus, there is competition between the host and the pathogen for the limited amount of micronutrients. Pathogens have also evolved sophisticated machinery to precisely balance the fine line between acquiring essential micronutrients (Fe, Zn, Cu, Mg, etc.) and at the same time defending against micronutrient excess. Thus, pathogens must maintain proper micronutrient homeostasis for successful pathogenesis.

Among the micronutrients, magnesium (Mg) is one of the crucial elements for *C. albicans* that plays a significant role in cell signalling, energy production, oxidative phosphorylation, nucleic acid synthesis and glycolysis [3]. It has previously been shown that the antifungal activity of bovine pancreatic trypsin inhibitor (BPTI) and the metal chelator diethylenetriamine penta-acetic acid (DTPA) in inhibiting the growth of *C. albicans* is via hindrance of cellular Mg uptake [4,5]. However, a comprehensive study describing the cellular responses responsible for regulating drug resistance and virulence under Mg stress in *C. albicans* is still elusive. Thus, the aim of the present study was to determine the effect of Mg deprivation on drug susceptibility, antifungal targets, morphogenesis and virulence determinants of *C. albicans*. Here we

* Corresponding authors.
E-mail addresses: drzeeshanfatima@gmail.com (Z. Fatima), saifhameed@yahoo.co.in (S. Hameed).

https://doi.org/10.1016/j.jgar.2019.01.011
2213-7165/

Table 1
List of *Candida albicans* strains used in the study.

Name	Genotype/detail	Reference
C. albicans	SC5314	[6]
DAY185	URA3/ura3Δ:λimm434 HIS1/his1:hisG ARG4/arg4:hisG	[18]
JRB64 (Δ*cnb1*/Δ*cnb1*)	ura3Δ:λimm434/ura3Δ:λimm434his1:hisG:HIS1/his1:hisGarg4:hisG/arg4:hisGcnb1:UAU1/cnb1:ARG4	[18]
YAG237 (*CNB1-1*/*CNB1*)	CNB1 mutant having hyperactive allele	[18]
GU4	Fluconazole-susceptible clinical isolate	[15]
GU5	Fluconazole-resistant strain derived from GU4 due to overexpression of CDR1	[15]
CDR1-GFP	AD1–8u cells harbouring CaCDR1-GFP integrated at the PDR5 locus	[16]
MDR1-GFP	AD1–8u cells harbouring CaMDR1-GFP integrated at the *PDR5* locus	[17]
Act1-GFP	Constitutive expression gene of Act1p integrated at the *RPS1* locus	[20]
MRC 10	ura3/ura3 icl1Δ:hisG/ura3:hisG RPS 10/rps10:Clp10-URA3	[19]
MRC 11	ura3/ura3 icl1Δ:hisG/ura3:hisG RPS 10/rps10:Clp10-ICL1-URA3	[19]

report that Mg availability is a crucial factor in drug resistance mechanisms in *C. albicans*.

2. Materials and methods

YPD (yeast extract–peptone–dextrose) medium, horse serum, nutrient broth, propidium iodide (PI), agar, thiazolyl blue tetrazolium bromide (MTT), bovine serum albumin (BSA) fraction V, rhodamine 6G (R6G), *N*-acetyl-D-glucosamine (NAG) and brain–heart infusion (BHI) were purchased from HiMedia (Mumbai, India). Mannitol, disodium hydrogen orthophosphate (Na_2HPO_4), potassium dihydrogen orthophosphate (KH_2PO_4), d-glucose, calcium chloride ($CaCl_2$), dimethyl sulfoxide (DMSO), potassium hydroxide (KOH), glycerol, *n*-heptane, sodium dodecyl sulfate (SDS), sodium acetate, sodium citrate, glucose, magnesium chloride ($MgCl_2$), potassium chloride (KCl) and cholesterol were obtained from Thermo Fisher Scientific (Waltham, MA). Nystatin, fluconazole (FLU), amphotericin B (Amp B), caspofungin (CAS), calcofluor white (CFW), crystal violet (CV) and trans-1,2-diaminocyclohexane tetra-acetic acid (CDTA) were obtained from Sigma Chemical Co. (St Louis, MO).

2.1. Growth media and establishment of magnesium deprivation

The *Candida* strains used in the study are listed in Table 1. Strains were cultured in YPD broth [yeast extract 1% (w/v), peptone 2% (w/v) and dextrose 2% (w/v)]. For the glyoxylate cycle, cells were grown in yeast nitrogen base (YNB) containing 0.67% YNB and 2% agar (for solid plates) supplemented with different carbon sources,

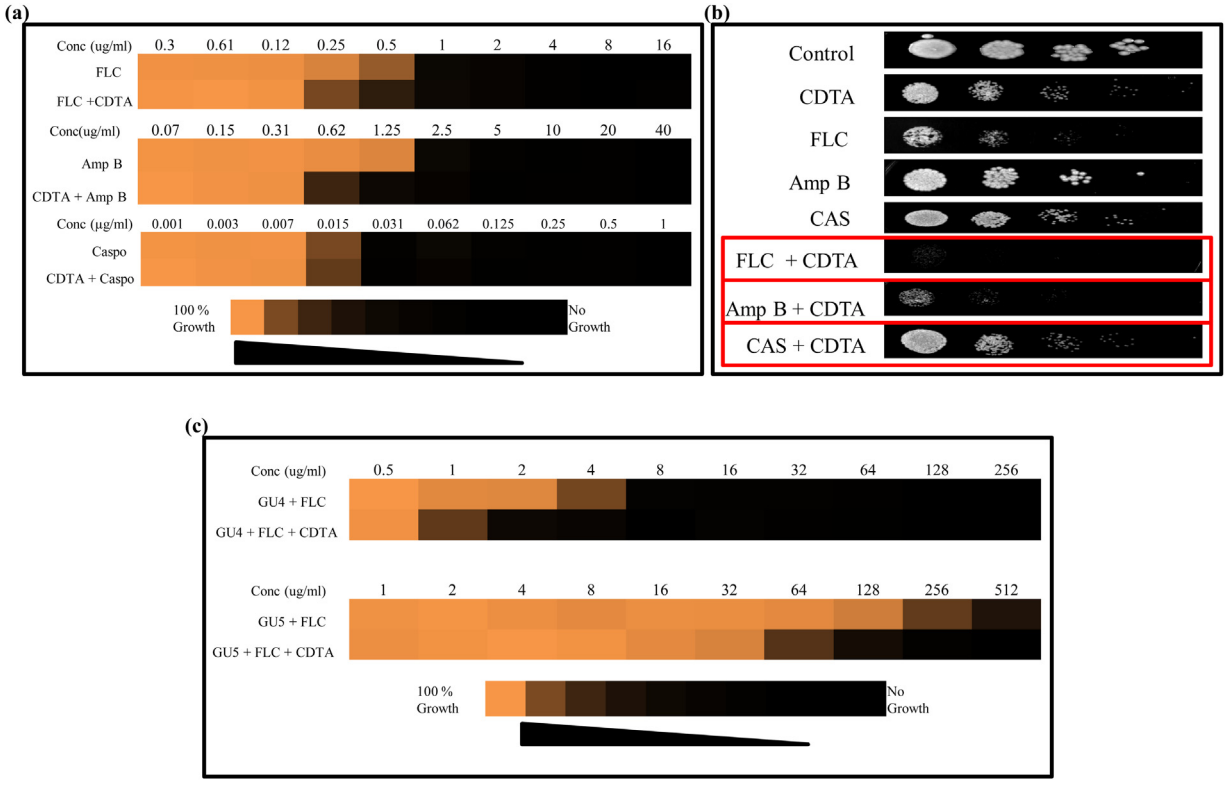

Fig. 1. Drug susceptibility assay of known antifungal drugs under magnesium (Mg) deprivation. (a) Minimum inhibitory concentrations (MICs) of *Candida albicans* SC5314 were determined by broth microdilution (BMD) for fluconazole (FLU), amphotericin B (Amp B) and caspofungin (CAS) alone (MICs of 0.5, 2.5 and 0.015 µg/mL, respectively) and in the presence of trans-1,2-diaminocyclohexane tetra-acetic acid (CDTA) (MICs of 0.25, 0.62 and 0.015 µg/mL, respectively) to ascertain the effect of Mg deprivation on susceptibility of FLU, Amp B and CAS. Data are shown quantitatively by colour (see colour bar below), where each shade of colour represents virtual optical densities of the cell. (b) Spot assay of *C. albicans* SC5314 in the presence FLU, Amp B and CAS (1, 2.5 and 0.1 µg/mL) alone and in the Mg-deprived condition. (c) BMD to determine the FLU MICs of *C. albicans* Gu4 and Gu5 (MICs of 4 µg/mL and 256 µg/mL) and in the presence of CDTA (MICs of 1 µg/mL and 64 µg/mL).

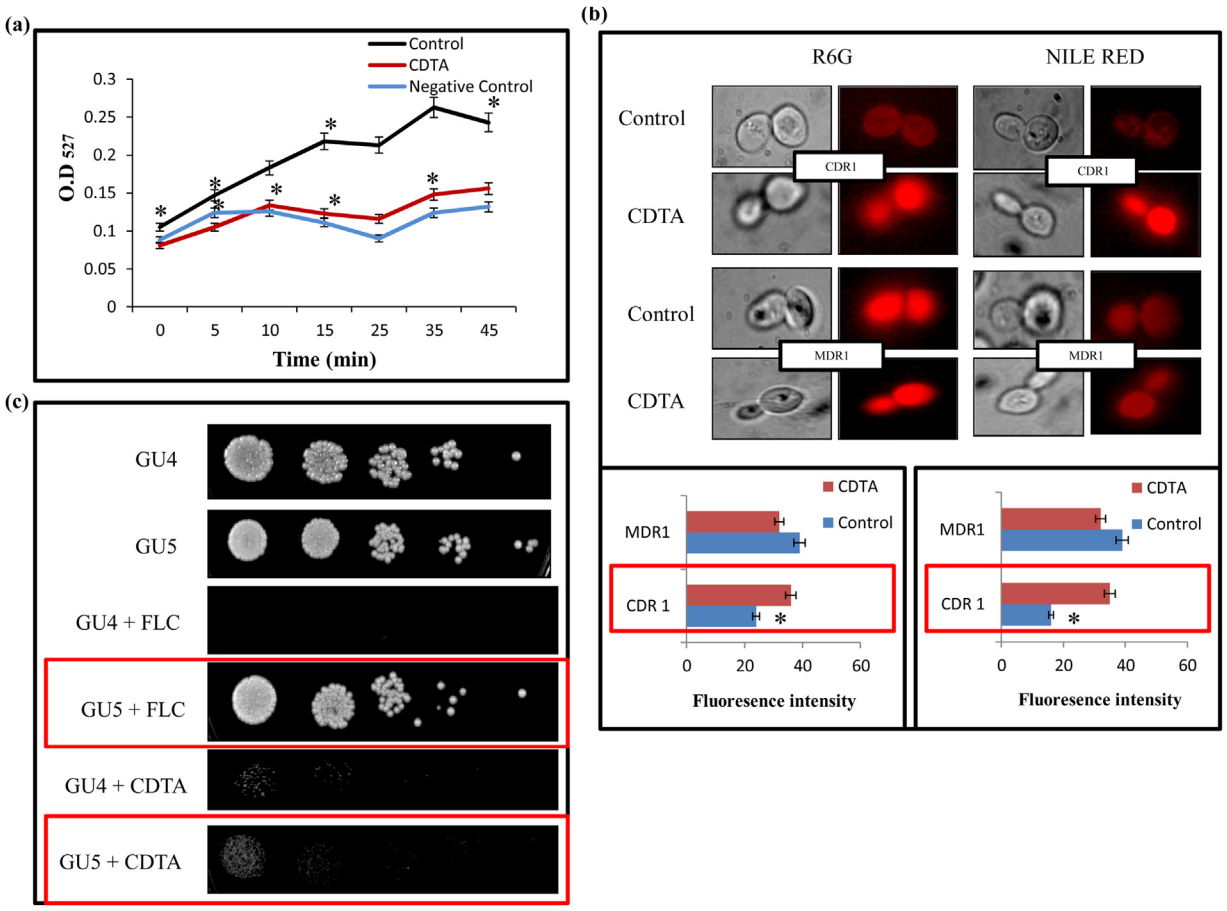

Fig. 2. Effect of magnesium (Mg) deprivation on the activity of the Cdr1p ABC transporter. (a) Efflux pump activity was estimated by extracellular concentrations of rhodamine 6G (R6G) in *Candida albicans* SC5314 cells grown in the absence (control) and presence of trans-1,2-diaminocyclohexane tetra-acetic acid (CDTA) (150 μg/mL). The negative control represents *C. albicans* SC5314 de-energised cells without glucose. The mean ± standard deviation optical density at 527 nm (OD_{527}) from three independent sets of experiments is depicted on the *y*-axis with respect to time (min) on the *x*-axis. $^{*}P < 0.05$. (b) R6G and Nile red accumulation assay (upper panel) in Cdr1p- and Mdr1p-overexpressing cells under Mg deprivation. The lower panel depicts fluorescence intensity measured by ImageJ software, represented as a bar graph. $^{*}P < 0.05$. (c) Spot assay for fluconazole (FLU) of Gu4 and Gu5 under Mg deprivation.

including 2% glucose, 2% citrate, 2% acetate, 5% ethanol or 2% glycerol. Cells were freshly revived in YPD broth and were transferred to an agar plate. Cells were grown at 30 °C on an agar plate before each study to ensure the revival of strains. CDTA, a well known Mg chelator, was used to establish Mg deprivation, which was confirmed by atomic absorption spectroscopy (Supplementary Fig. S1a). Growth reversion with Mg confirmed that CDTA was efficient enough to chelate Mg (Supplementary Fig. S1b). Since Mg is an essential micronutrient required for the growth of numerous micro-organisms, including *C. albicans* SC5314 [6], it was necessary to ensure that only a concentration of CDTA that does not cause any appreciable growth defect was used. This was achieved by two different methods, namely the spot assay and growth curve. *Candida* growth was completely inhibited at a concentration of 175 μg/mL CDTA, whereas at 150 μg/mL growth was not substantially affected (Supplementary Fig. S1c). A CDTA concentration of 150 μg/mL was also confirmed by growth curve in the presence of Mg deprivation, which was in accordance with the spot assay (Supplementary Fig. S1d). These results confirmed that CDTA at a concentration of 150 μg/mL was subinhibitory enough to show a partial inhibitory effect on *C. albicans* SC5314. Thus, for subsequent biochemical and phenotypic studies, CDTA at this subinhibitory concentration of 150 μg/mL was used.

2.2. Drug susceptibility testing

Drug susceptibility was tested by broth microdilution (BMD) and spot assay, as described below.

2.2.1. Minimum inhibitory concentration (MIC) determination

The MIC was determined by the BMD method as described by the Clinical and Laboratory Standards Institute (CLSI) [7]. For FLU and CAS, the MIC was calculated as the MIC_{50}, while for Amp B the MIC was calculated as the MIC_{100}.

2.2.2. Spot assay

The spot assay was performed using a previously described method [8,9] in the absence (control) and presence of a Mg-deprived condition. Briefly, 5 μL of five-fold serially diluted yeast cultures [optical density at 600 nm (OD_{600}) = 0.1] were spotted onto YPD plates. The growth difference was measured after 48 h at 30 °C. The concentrations used in this study are specified in the figure legends.

2.3. Rhodamine 6G efflux

Efflux of R6G was determined using a previously described protocol [10,11] with approximately 1×10^6 yeast cells from an overnight-grown culture in the absence (control) and presence of CDTA (150 μg/mL). Energy-dependent efflux (at the indicated time) was measured with glucose (2%) and absorption was measured at 527 nm. Glucose-free negative controls were included in all experiments.

2.4. Propidium iodide influx

The cell membrane is impermeable to PI dye, which is widely used to differentiate viable cells as described previously [12]. To evaluate the effect of Mg deprivation, *C. albicans* SC5314 cells (approximately 1×10^3 CFU/mL) were obtained from exponential phase and were exposed to CDTA (150 μg/mL) for 3 h at 30 °C with gentle shaking. Cells were then harvested, were incubated with PI for 15 min and were observed by fluorescence microscopy (Coslab, Ambala, India).

2.5. Ergosterol quantitation

Sterols were extracted by the alcoholic KOH method and the percentage ergosterol was calculated as described previously [8,12]. *C. albicans* SC5314 cells were inoculated in 50 mL of YPD in the absence (control) or presence of CDTA (150 μg/mL). Both ergosterol and 24(28)-dehydroergosterol (DHE) absorb at 281.5 nm, whereas only 24(28)-DHE absorbs at 230 nm. The ergosterol content was determined by subtracting the amount of 24(28)-DHE (calculated from the OD_{230}) from the total ergosterol plus 24(28)-DHE content (calculated from the $OD_{281.5}$).

2.6. Isocitrate lyase (ICL1) and malate synthase (MLS1) enzyme assay

C. albicans SC5314 cells were grown in YNB medium under Mg deprivation supplemented with 2% acetate to trigger the expression of glyoxylate cycle enzymes. Cells were harvested by centrifugation at 5000 × *g* for 3 min. Cell-free extract was prepared as described previously [13]. Briefly, cells were washed once with lysis buffer

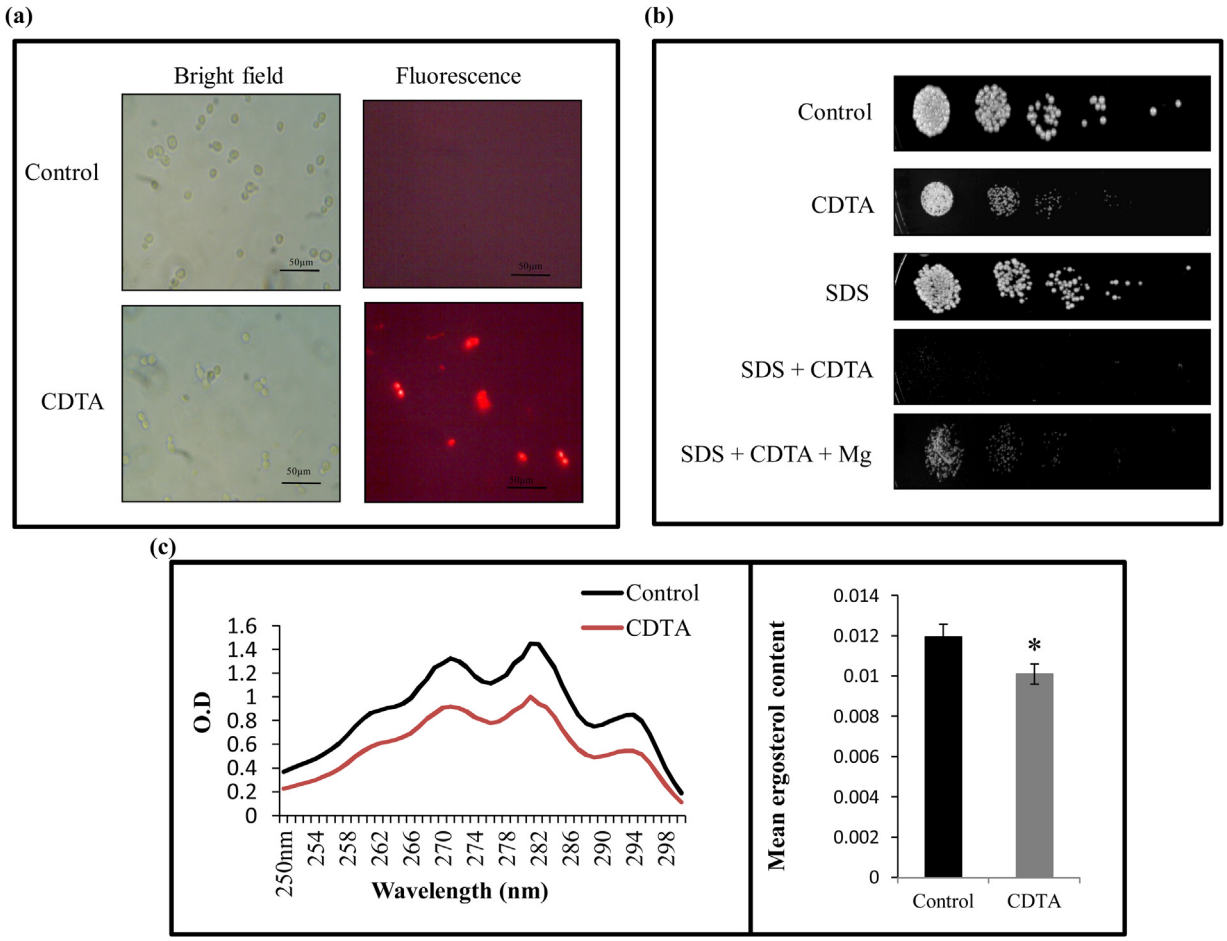

Fig. 3. Effect of magnesium (Mg) deprivation on the *Candida albicans* cell membrane. (a) Fluorescence microscopy of propidium iodide (PI)-stained *C. albicans* SC5314 cells (red fluorescence) under Mg deprivation at 40× magnification. (b). Spot assay of *C. albicans* SC5314 cells in the absence (control) and presence of trans-1,2-diaminocyclohexane tetra-acetic acid (CDTA) (150 μg/mL) with the membrane-perturbing agent sodium dodecyl sulfate (SDS) (0.02%). (c) Left panel shows ultraviolet spectrophotometric ergosterol profiles of *C. albicans* SC5314 scanned between 220 nm and 300 nm from an overnight culture grown with and without CDTA (150 μg/mL). The right panel shows relative percentages of ergosterol content in the absence (control) and presence of CDTA (150 μg/mL). The mean ± standard deviation ergosterol level (%), calculated as described in Section 2.5 normalised by considering the untreated control as 100, of three independent sets of experiments is depicted on the *y*-axis. $^*P < 0.05$.

[100 mM potassium phosphate buffer (pH 7.5), 2 mM $MgCl_2$, 1 mM dithiothreitol (DTT)] and were centrifuged again at 5000 × *g* for 3 min to collect the cell pellet. The cell pellet was then re-suspended with the same lysis buffer and was sonicated for 3 min. The cell lysate was centrifuged at 14 000 × *g* at 4 °C for 30 min to obtain the cell-free supernatant that was directly used in the enzyme assay. The 1-mL reaction volume contained 25 mM imidazole (pH 6.8), 5 mM $MgCl_2$, 1 mM ethylene diamine tetra-acetic acid (EDTA), 4 mM phenylhydrazine hydrochloride, 1 mM dl-isocitric acid (substrate) and cell-free extract. The reaction starts immediately after the addition of substrate. Glyoxylate phenylhydrazone formation was assessed spectrophotometrically at 324 nm using a VSI-501 UV–vis spectrophotometer (ScientificBazaar™, Chandigarh, India) following incubation at 30 °C to determine ICL activity in the reaction for the subsequent inhibition study. For MLS1 activity, the 1-ml reaction volume contained 50 mM imidazole (pH 6.8), 100 mM $MgCl_2$, 2.5 mM acetyl CoA, 10 mM glyoxylic acid solution, 0.2 mM 5,5'-dithiobis-(2-nitrobenzoic acid) (DTNB) solution, 95% ethanol and cell-free extract. The reaction starts immediately after the addition of substrate. 5-Thio-2-nitrobenzoic acid formation was assessed spectrophotometrically at 412 nm using a VSI-501 UV–vis spectrophotometer following incubation at 30 °C to determine the MLS enzyme activity in the reaction.

2.7. Yeast-to-hyphal transition

Hyphal induction of *C. albicans* SC5314 was performed on hyphal induction medium such as 10% (v/v) horse serum and Spider (1% nutrient broth, 1% mannitol, 0.2% K_2HPO_4). Dimorphic switching was performed using the protocol described previously [9,12]. Following incubation, cells were transferred to the required medium for hyphal growth in the presence of CDTA, and hyphae were observed under a microscope at magnifications of 40× and 4× for liquid and solid media, respectively.

2.8. Biofilm formation and cell adherence

C. albicans SC5314 biofilms were established on the surface of 96-well polystyrene plates as previously described [8,9]. A cell suspension of 1×10^7 cells/mL was made in phosphate-buffered saline (PBS) and 100 μL was inoculated into each well. Plates were then incubated at 37 °C at 50 rpm for 90 min. Wells were washed to remove non-adherent cells. The biofilm was formed by suspending 200 μL of YPD medium along with CDTA (150 μg/mL) in 96-well polystyrene plates incubated at 37 °C for 24 h. Following incubation, biofilms were observed under a light microscope at 40× magnification. To monitor the metabolic activity of the biofilm and

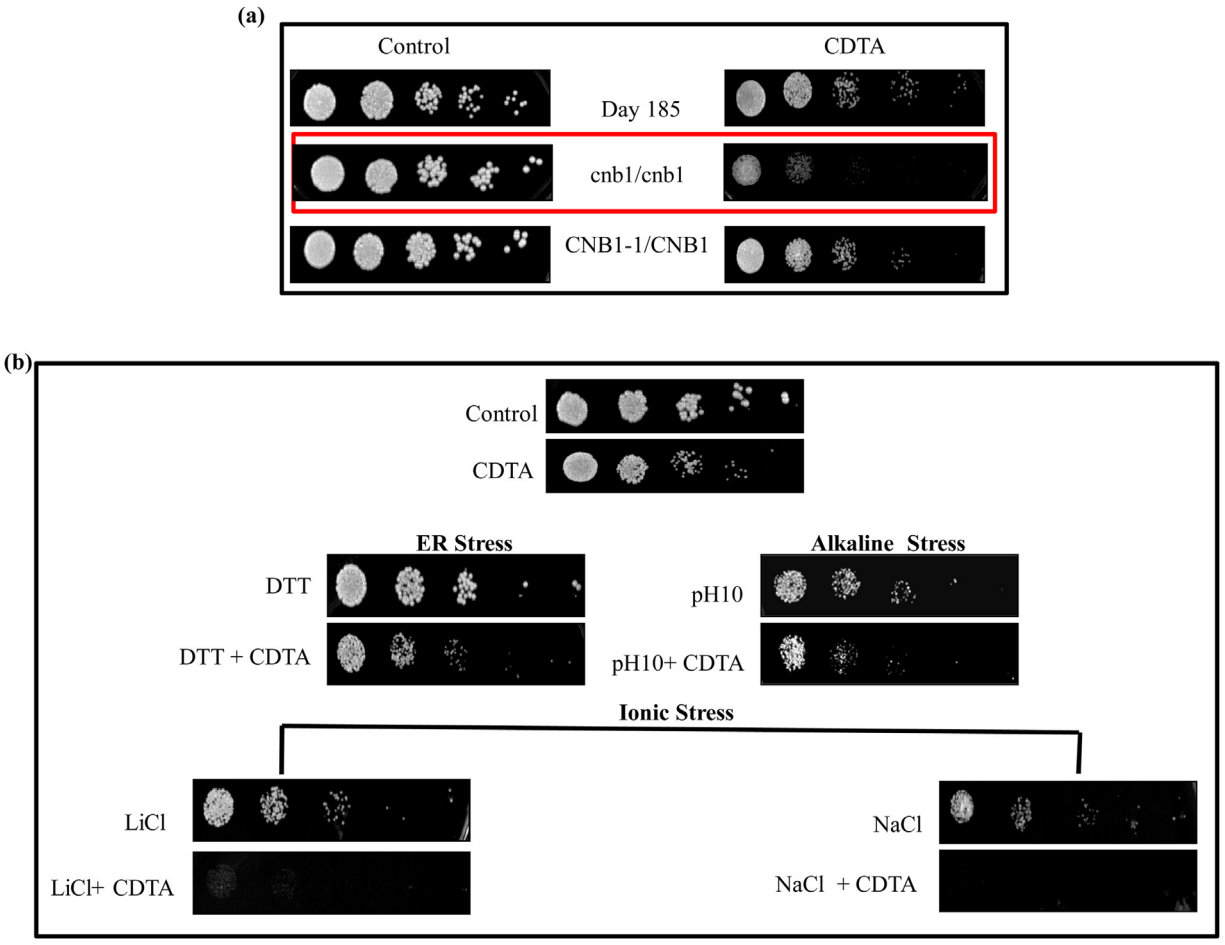

Fig. 4. Effect of magnesium (Mg) deprivation on calcineurin signalling. (a) Spot assay depicting loss of growth in Δ*cnb1* mutant in the presence of Mg deprivation (150 μg/mL), while the CNB1-1/CNB1 calcineurin-overexpressing strain grew efficiently in the presence of Mg deprivation. (b) Spot assays of *Candida albicans* SC5314 under various stresses, namely endoplasmic reticulum (ER) stress [20 mM dithiothreitol (DTT)], alkaline stress (pH 10) and ionic stress (LiCl 0.2 M and NaCl 1.5 M) with Mg-deprived condition (150 μg/mL).

for the cell adhesion assay (except that primarily treated and non-treated cells were grown to an OD_{600} of 1.0) on the surface of a 96-well polystyrene plate, MTT was added by 50 μL (stock solution containing 5 mg/mL) in each well. Plates were incubated for 5 h at 37 °C. DMSO (200 μL) was then added to each well to solubilise the MTT formazan product and the OD_{450} was measured. Biofilm biomass was measured as described previously [14] with slight modifications. Pre-weighed sterile silicone squares (1.5 × 1.5 cm) were pre-treated overnight with BSA and were washed with PBS before inoculation. Exponentially-grown *C. albicans* SC5314 cells were diluted to an OD_{600} of 0.2 with Spider medium and the suspension was added to a sterile 12-well plate with one prepared silicone square in each well. The inoculated plate was incubated at 37 °C for 90 min with gentle agitation (150 rpm) until adhesion occurred. The silicone squares were washed with PBS and were then moved to a fresh 12-well plate containing 2 mL of fresh Spider medium. The plate was incubated at 37 °C for an additional 60 h with agitation at 75 rpm to allow biofilm formation. For dry mass measurements, the total biomass of each biofilm was calculated by subtracting the pre-determined weight of the silicon squares.

2.9. Adherence to epithelial cells

An adherence assay was performed as described previously [9]. Yeast cells were grown in YPD broth for 24 h at 37 °C, were re-suspended in 2 mL of sterile PBS (pH 6.8) and were washed twice by centrifugation (3000 × *g*, 5 min). Adherence assays were developed by mixing 1 mL of each suspension in a test tube and incubating in the presence of CDTA at 37 °C under gentle stirring for 2 h. Following incubation, 0.4% of trypan blue solution was added to each tube and the mixture was gently shaken. Stained suspensions were examined under a light microscope at 40× magnification.

2.10. RNA isolation

Isolation of RNA from *C. albicans* SC5314 was performed using a combination of TRIzol and RNeasy Mini Kit with DNase (QIAGEN, Hilden, Germany) treatment [9]. Cells were diluted in 50 mL of fresh YPD broth at an OD_{600} of 0.1 (10^6 cells/mL) in the absence or presence of CDTA and were grown at 30 °C to an OD_{600} of 1.0. For reverse transcription PCR (RT-PCR), cDNA was synthesised with a RevertAid™ H Minus cDNA Synthesis Kit (Invitrogen, Waltham, MA) from the isolated RNA. The synthesised cDNA product (2 μL) was directly used for PCR amplification (50 μL) using gene-specific forward and reverse primers (Table 2). The amplified products were gel electrophoresed and the densities of bands (for genes of interest) were measured and quantified by normalising to that of the constitutively expressed actin gene (*ACT1*).

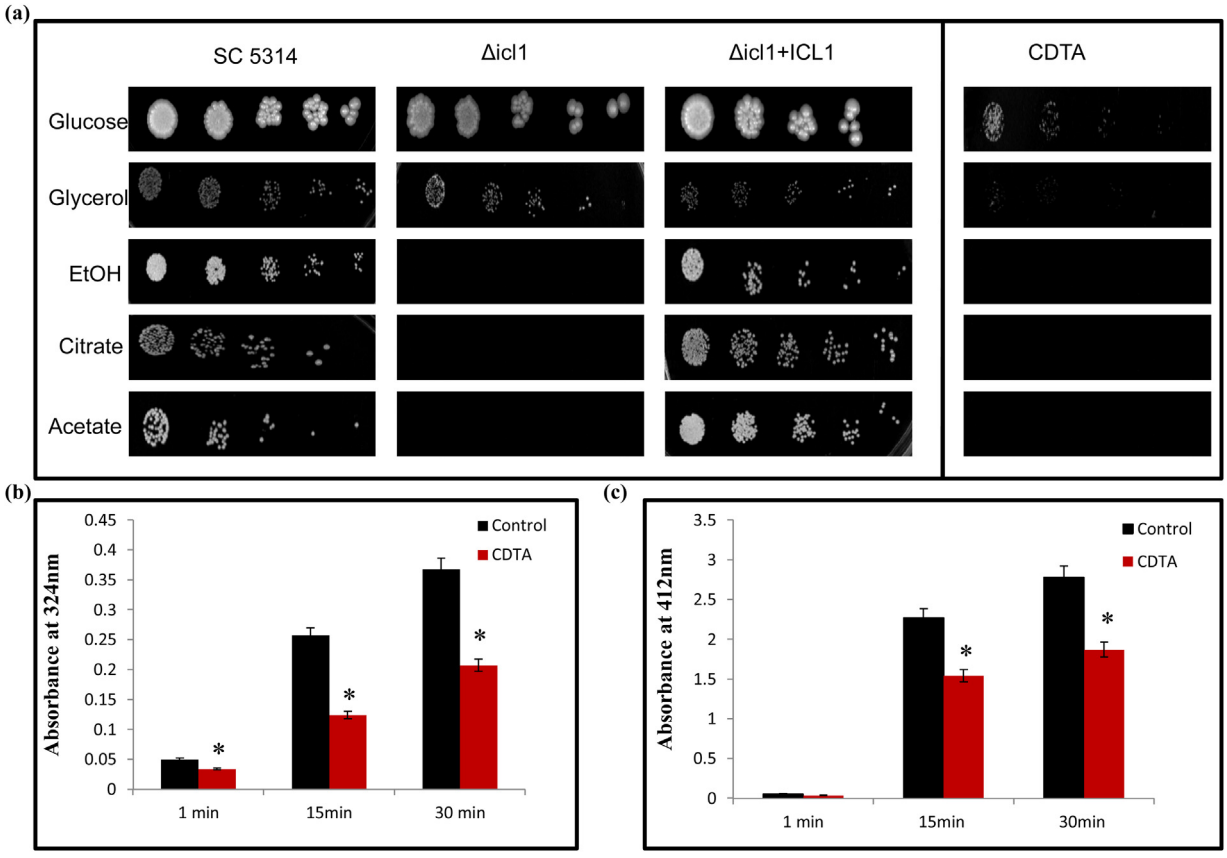

Fig. 5. Effect of magnesium (Mg) deprivation on the glyoxylate cycle. (a) Spot assays of *Candida albicans* SC5314, MRC10 (Δ*icl1*) and MRC11 (Δ*icl1* + ICL1) cultured cells depicting loss of growth in the presence of trans-1,2-diaminocyclohexane tetra-acetic acid (CDTA) (150 μg/mL) under different carbon sources (2% glucose, 2% glycerol, 2% ethanol, 2% sodium citrate and 2% sodium acetate). (b) Isocitrate lyase (ICL1) enzyme activity of *C. albicans* SC5314 in the presence of CDTA. Mean enzyme activity of ICL1 expressed as absorbance at 324 nm± SD is depicted on Y axis and * depicts P value <0.05. (c) Malate Sy-axis. *$P < 0.05$. (c) Malate synthase (MLS1) enzyme activity of *C. albicans* SC5314 in the presence of CDTA. Mean enzyme activity of MLS1 expressed as absorbance at 412 nm is depicted on the *y*-axis. *$P < 0.05$. Each data point represents the mean ± standard deviation of three experiments.

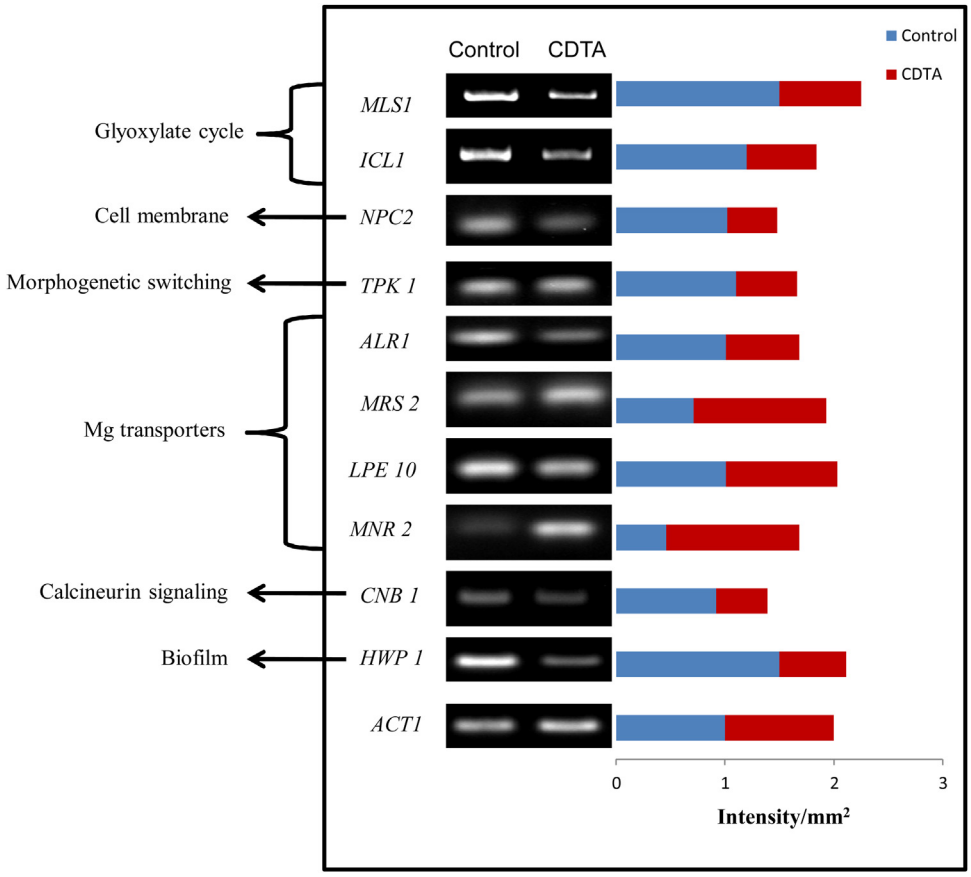

Fig. 6. Reverse transcription PCR (RT-PCR) under magnesium deprivation. The leftshow transcript levels *Candida albicans* SC5314 of *MLS1*, *ICL1*, *NPC2*, *TPK1*, *ALR1*, *MRS2*, *LPE10*, *MNR2*, *CNB1* and *HWP1*: lane 1, control; lane 2, trans-1,2-diaminocyclohexane tetra-acetic acid (CDTA) (150 μg/mL). The right-hand panel shows the quantitation (density expressed as intensity/mm^2) of the respective transcripts normalised to the constitutively expressed *ACT1* transcript.

2.11. Maintenance and survival of Caenorhabditis elegans

Nematodes were handled according to previously described methodology [13]. *C. elegans* strain N2 was maintained and propagated on *Escherichia coli* strain OP50. Approximately 30 *C. elegans* L4 stage or young adult hermaphrodites were transferred from a lawn of *E. coli* OP50 to BHI medium with CDTA (25 μg/mL). Worms were considered dead when they did not respond to tapping on the plate and were scored on a daily basis. Nematode survival was plotted using the Kaplan–Meier method.

For the *C. elegans* co-infection liquid assay, a previously described methodology was used [13]. Nematodes were sequentially pre-infected with *C. albicans* SC5314 for 2 h on BHI agar medium, were washed with M9 buffer and were transferred to wells (30 worms per well) of a 12-well microtitre dish containing 2 mL of liquid medium (20% BHI and 80% M9 buffer) with or without a Mg-deprived condition. Dishes were incubated for 7 days at 25 °C and images were taken at 10× with a Coslab camera. For the persistence assay, *C. albicans* SC5314 and Act1p-GFP lawns were prepared and worms were placed for 6 h and then pipetted onto nematode growth medium plates. *C. albicans* SC5314-fed *C. elegans* were stained with CFW on the second day of infection. Fluorescence of Act1p-GFP- and CFW-stained *C. albicans* was observed under Mg deprivation in the proximal and distal intestine of *C. elegans* using a Coslab fluorescence microscope.

Table 2
List of primers used for reverse transcription PCR (RT-PCR) in the study.

Gene name	Primer sequence
ACT1	F, TTTTGACCTTGAGATACCCA
	R, GGAGCTCTGAATCTTTCGTT
CNB1	F, ATGGGGGCTAATGCAAGTAT
	R, AATGTCAAAGTGTTGGCAAT
NPC2	F, GAACTTGGCAATTGTTACCC
	R, CAGGGAATATAATTGTAGCAG
TPK1	F, ATGGAACCAGCAGACACAA
	R, CCCCCACATTCGAATTAT
HWP1	F, ACTACCCACAACAACCACAA
	R, GCAGATGATGATTCTGAAGTG
ALR1	F, TGGTGGTGATGGTAGTAGTGG
	R, TTCACGAGTTTCTTGCATTCG
MRS2	F, TGATTCGACCTTCAAGTGCA
	R, TTTCTATTGGCGTCGAGGAT
LPE10	F, TCAGCAACAGGAACAACAACA
	R, TCGTGGTTGTCCATCACCTT
MNR2	F, AGCACCGTTGACCAAGTCG
	R, TTAATTGGATGAGGGGTTGC
ICL1	F, CAATCATTGCTGATGCTGACA
	R, TTCTCTGGCTCTGGCAACAT
MLS1	F, ATTGACCCCAGCTTGGAAAA
	R, GCCAAAGCAGCTCTGTTTCTT

2.12. Statistical analysis

All experiments were performed in triplicate and the results are reported as the mean ± standard deviation. Data were analysed by

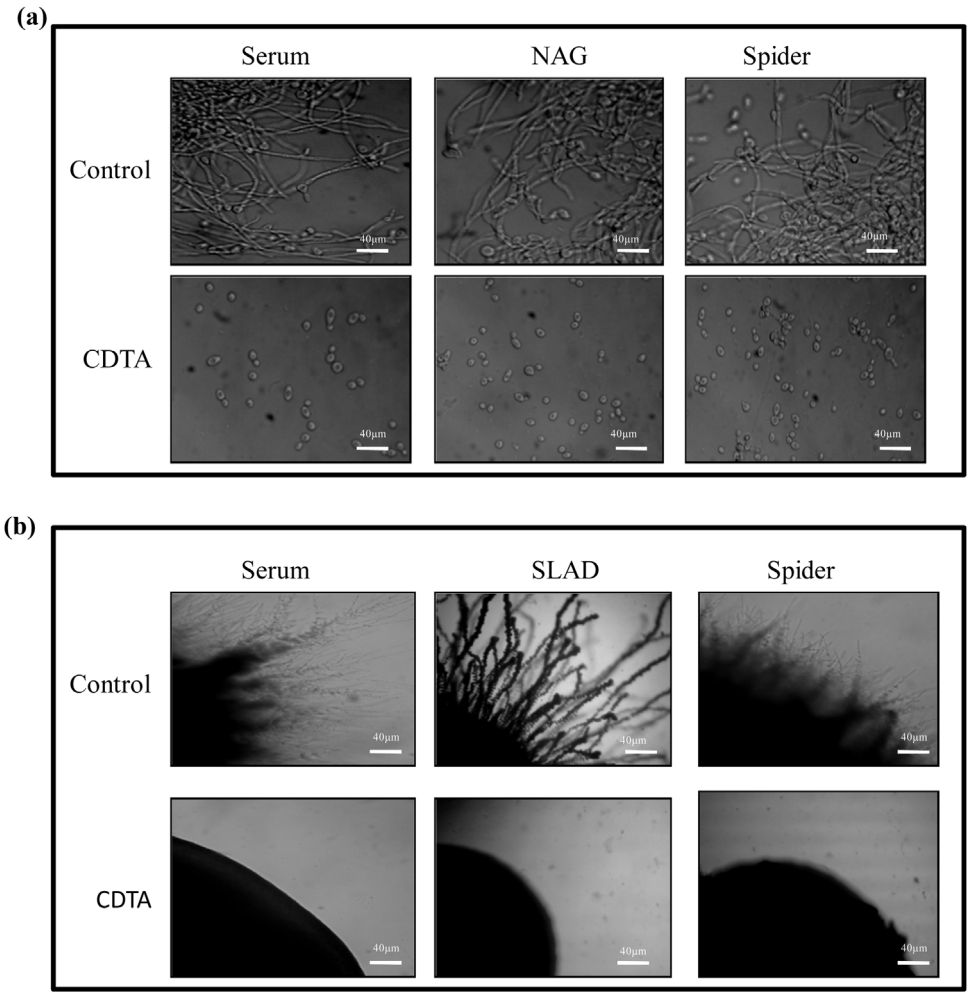

Fig. 7. Effect of magnesium deprivation on hyphal morphogenesis. (a) Hyphal morphogenesis in liquid hyphae-inducing media [10% serum, *N*-acetyl-d-glucosamine (NAG) and Spider medium] in the absence (control) and presence of trans-1,2-diaminocyclohexane tetra-acetic acid (CDTA) (150 μg/mL) in *Candida albicans* SC5314 at 4 h (magnification 40×). (b) Hyphal morphogenesis in solid hyphae-inducing media [10% serum, synthetic low-ammonium–dextrose (SLAD) medium and Spider medium] in the absence (control) and presence of CDTA (150 μg/mL) in *C. albicans* SC5314 at 4 h (magnification 4×).

Student's *t*-test, and a *P*-value of <0.05 was considered statistically significant.

3. Results

3.1. Magnesium deprivation potentiates the antifungal activity of membrane-targeting drugs

The effects of Mg deprivation on the susceptibility of *C. albicans* to major antifungal classes, namely azoles, polyenes and echinocandins, were studied. First, a drug susceptibility assay was performed with antifungal drugs (FLU, Amp B and CAS) without Mg deprivation. The MICs of the tested drugs were 0.5, 2.5 and 0.015 μg/mL, respectively (Fig. 1a). Mg deprivation led to increased susceptibility only to FLU (MIC = 0.25 μg/mL) and Amp B (MIC = 0.62 μg/mL), with no effect on the MIC of CAS (Fig. 1a). These results were further evaluated by spot assay, which was consistent with BMD (Fig. 1b). In addition, the MICs of a matched pair of clinical isolates (Gu4 and Gu5) [15] under Mg deprivation were tested. The MIC of the FLU-susceptible strain Gu4 decreased from 4 μg/mL to 1 μg/mL and the MIC of the FLU-resistant strain Gu5 decreased from 256 μg/mL to 64 μg/mL (Fig. 1c).

3.2. Magnesium deprivation affects efflux pump activity

Next, the functionality of efflux pumps under Mg deprivation was examined by monitoring R6G efflux and it was observed that Mg deprivation led to abolished R6G efflux (Fig. 2a). Furthermore, to validate the above results, accumulation of R6G (a substrate for Cdr1p) and Nile red (a substrate for both Cdr1p and CaMdr1p) was examined [16,17] in order to explore whether the effect of Mg deprivation was specific to any particular transporter family, such as ATP binding cassette (ABC) or major facilitator superfamily (MFS). It was observed that both R6G and Nile red were able to accumulate more in Cdr1p-overexpressing cells under Mg-deprived condition compared with Mdr1-overexpressing cells (Fig. 2b). In addition, growth of a matched pair of clinical isolates overexpressing Cdr1p was examined and it was found that Mg deprivation rendered the resistant strain Gu5 hypersensitive to FLU (Fig. 2c).

3.3. Magnesium deprivation leads to perturbed membrane homeostasis

PI is a well-known fluorescent dye that binds to nucleic acid only when the membrane is not intact. The results of this study

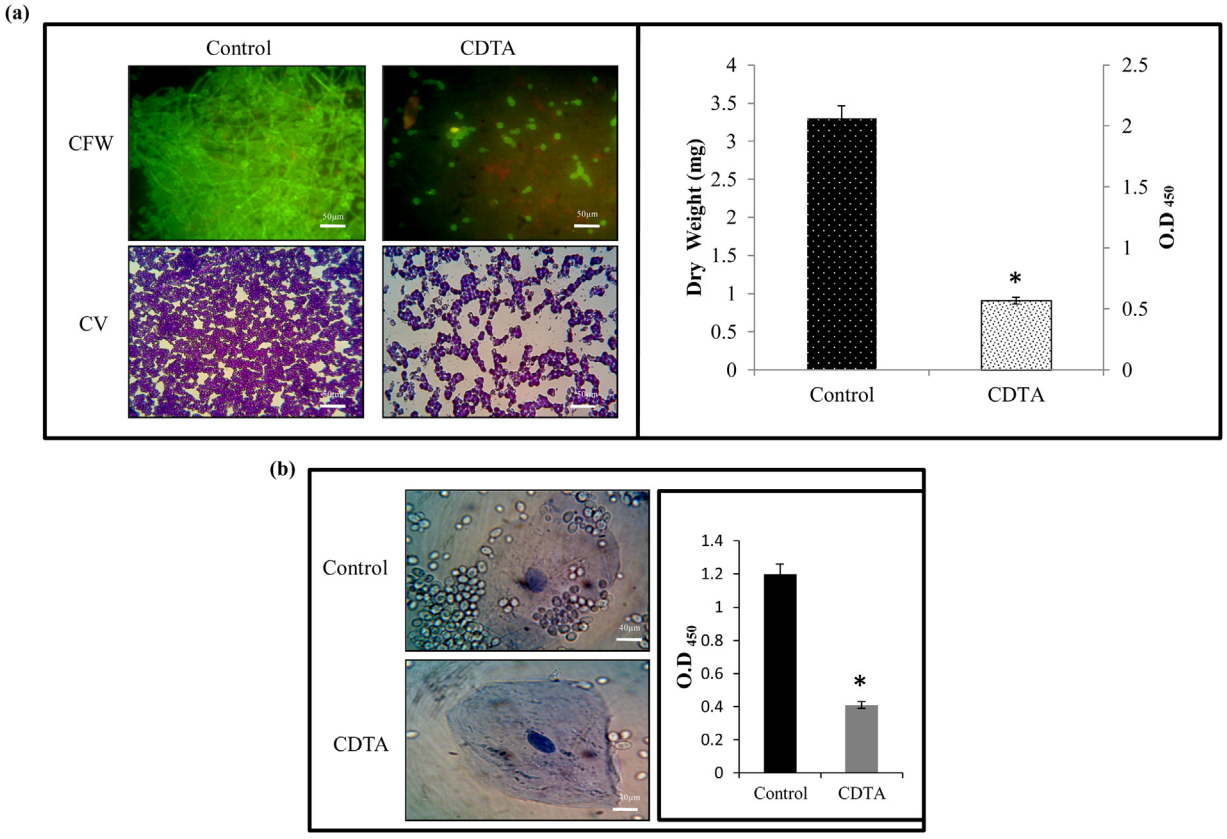

Fig. 8. Mg deprivation on biofilm formation and cell adherence. (a) The left panel show calcofluor white (CFW) and crystal violet (CV) staining of *Candida albicans* SC5314 showing biofilm formation in the absence (control) and presence of trans-1,2-diaminocyclohexane tetra-acetic acid (CDTA) (150 μg/mL). The right panel depicts biofilm formation and biomass depicted as a bar graph and quantified using MTT assay and dry weight (mg) measurement, respectively. Data are expressed as the mean ± S.D. of three independent sets of experiments. $^{*}P < 0.05$. (b) The left panel displays the effect of CDTA on adherence of *C. albicans* SC5314 to human oral epithelial cells. In the absence of CDTA (control), *C. albicans* SC5314 cells appeared adhered to the human oral epithelial cells, whereas in the presence of CDTA (150 μg/mL) *C. albicans* SC5314 did not adhere to the epithelial cells. The right panel displays the effect of CDTA on the adherence of *C. albicans* SC5314 to a polystyrene surface, which was quantified using MTT assay. Data are expressed as mean ± S.D. of three independent sets of experiments. $^{*}P < 0.05$. S.D., standard deviation.

revealed enhanced fluorescence under Mg deprivation, confirming a disrupted membrane (Fig. 3a). In addition, phenotypic susceptibility in the presence of SDS was determined and it was observed that Mg-deprived cells were hypersensitive in the presence of SDS (Fig. 3b). Furthermore, the level of ergosterol, one of the main components of the cell membrane, was estimated. There was a distinct decline ($P < 0.05$) in ergosterol levels under Mg deprivation (Fig. 3c). All of these observations suggested that Mg deprivation leads to disruption of cell membrane homeostasis.

3.4. Magnesium deprivation affects the calcineurin signalling pathway

To verify the effect of Mg deprivation on calcineurin signalling, a calcineurin mutant [18] that was susceptible under Mg-deprived condition was used (Fig. 4a). Furthermore, a phenotypic susceptibility assay was performed with different stress conditions such as DTT (endoplasmic reticulum stress), pH 10 (alkaline stress), and LiCl and NaCl (ionic stress) that require intact calcineurin signalling. As expected, it was observed that cells were susceptible under all calcineurin-dependent stress conditions under Mg deprivation (Fig. 4b). Thus, we hypothesise that Mg deprivation affects the calcineurin signalling pathway.

3.5. Magnesium deprivation leads to inhibition of the glyoxylate cycle

To explore the effect of Mg deprivation on the glyoxylate cycle, the drop dilution assay was performed with different non-fermentable carbon sources such as glycerol, ethanol, citrate and acetate. As expected, the *ICL1* knockout mutant (Δ*icl1*) was hypersensitive under all low-carbon conditions, which could be rescued in the revertant strain of *ICL1* [19]. Interestingly, under Mg deprivation it exhibits hypersensitivity similarly to the Δ*icl1* mutant (Fig. 5a). This suggest that Mg deprivation leads to interference in glyoxylate cycle functioning. For further confirmation, the enzymatic activity and transcript levels of *ICL1* and *MLS* were estimated. Interestingly, both enzyme activities (Fig. 5b,c) and transcript levels (Fig. 6) were inhibited under Mg deprivation. All of these results confirmed that the Mg-deprived condition leads to impaired metabolic flexibility in *C. albicans* SC5314.

3.6. Magnesium deprivation inhibits potential virulence traits

3.6.1. Inhibition of hyphal morphogenesis

The effect of Mg deprivation on yeast-to-hyphal transition in *C. albicans* SC5314 was further tested. Under the Mg-deprived

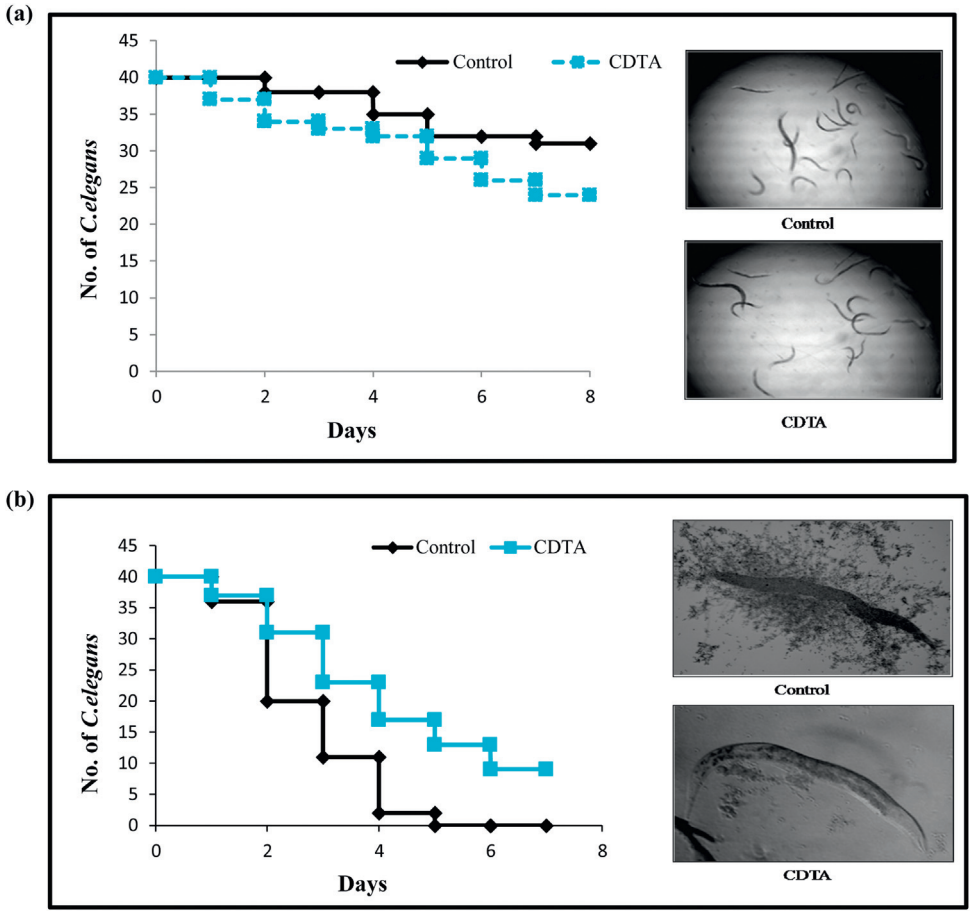

Fig. 9. Effect of magnesium (Mg) deprivation on the fungal-infected nematode model of *Caenorhabditis elegans*. (a) The toxicity of trans-1,2-diaminocyclohexane tetra-acetic acid (CDTA) (25 μg/mL) was studied in non-infected nematodes by determining survival rates after 7 days. (b) Kaplan–Meier graph depicting survival of *C. elegans* on exposure of *Candida albicans* SC5314-infected nematodes under Mg deprivation (CDTA 25 μg/mL).

condition, hyphal transition was significantly inhibited in all hyphae-inducing conditions both in liquid media, namely serum, NAG and Spider medium (Fig. 7a), and in solid media, namely serum, synthetic low-ammonium–dextrose (SLAD) medium and Spider medium (Fig. 7b). This observation suggests that Mg deprivation affects the yeast-to-hyphal transition in *C. albicans* SC5314.

3.6.2. Inhibition of biofilm formation and cell adherence

To study the effect of Mg deprivation on biofilm formation, first qualitative testing was performed and biofilms were visualised by staining with two different dyes (CFW and CV). Biofilm formation was inhibited in the presence of the Mg-deprived condition (Fig. 8a). Inhibited biofilms were further validated by quantitative methods by estimating metabolic activity by the MTT assay and by measuring the biofilm biomass. Together, it was observed that the metabolic activity and biofilm biomass were inhibited up to 60% and 80%, respectively, in the Mg-deprived condition (Fig. 8a).

Next, an adherence assay of *C. albicans* SC5314 cells to human epithelial cells and a microtitre plate polystyrene surface was performed. Cell adherence of *C. albicans* cells was inhibited both on epithelial cells (Fig. 8b) and the microtitre plate polystyrene surface under Mg deprivation (Fig. 8b). These results clearly suggested that Mg deprivation inhibited biofilm formation as well as cell adherence in *C. albicans* SC5314.

3.7. RT-PCR validates abrogated biochemical phenotypes under magnesium deprivation

For validation of the above phenotypes, RT-PCR under similar growth conditions as used for all biochemical assays was performed. Ten genes from various phenotypic categories were randomly selected, including cell membrane (*NCP2*), morphological switching (*TPK1*), calcineurin signalling (*CNB1*), Mg transporters (*ALR1*, *MRS2*, *LPE10* and *MNR2*), biofilm (*HWP1*) and glyoxylate cycle (*ICL1* and *MLS1*). RT-PCR results revealed that all of the tested genes showed good correlation with the observed abrogated phenotypes under Mg deprivation (Fig. 6).

3.8. Enhanced survival of C. elegans under magnesium deprivation

C. elegans, a widely used nematode model, was examined to evaluate the toxicity and survival under Mg-deprived condition. First, the survival rate of *C. elegans* under Mg deprivation was studied and it was found that *C. elegans* were able to survive in the presence of CDTA at a concentration of 25 μg/mL for 8 days, similar to the untreated nematodes (Fig. 9a). This suggested that Mg deprivation at the abovementioned CDTA concentration was non-toxic to *C. elegans* and may be further used to study their survival with *C. albicans* SC5314 infection. The survival rate of infected worms was increased in the presence of the Mg-deprived condition compared with untreated worms. *C. albicans* SC5314

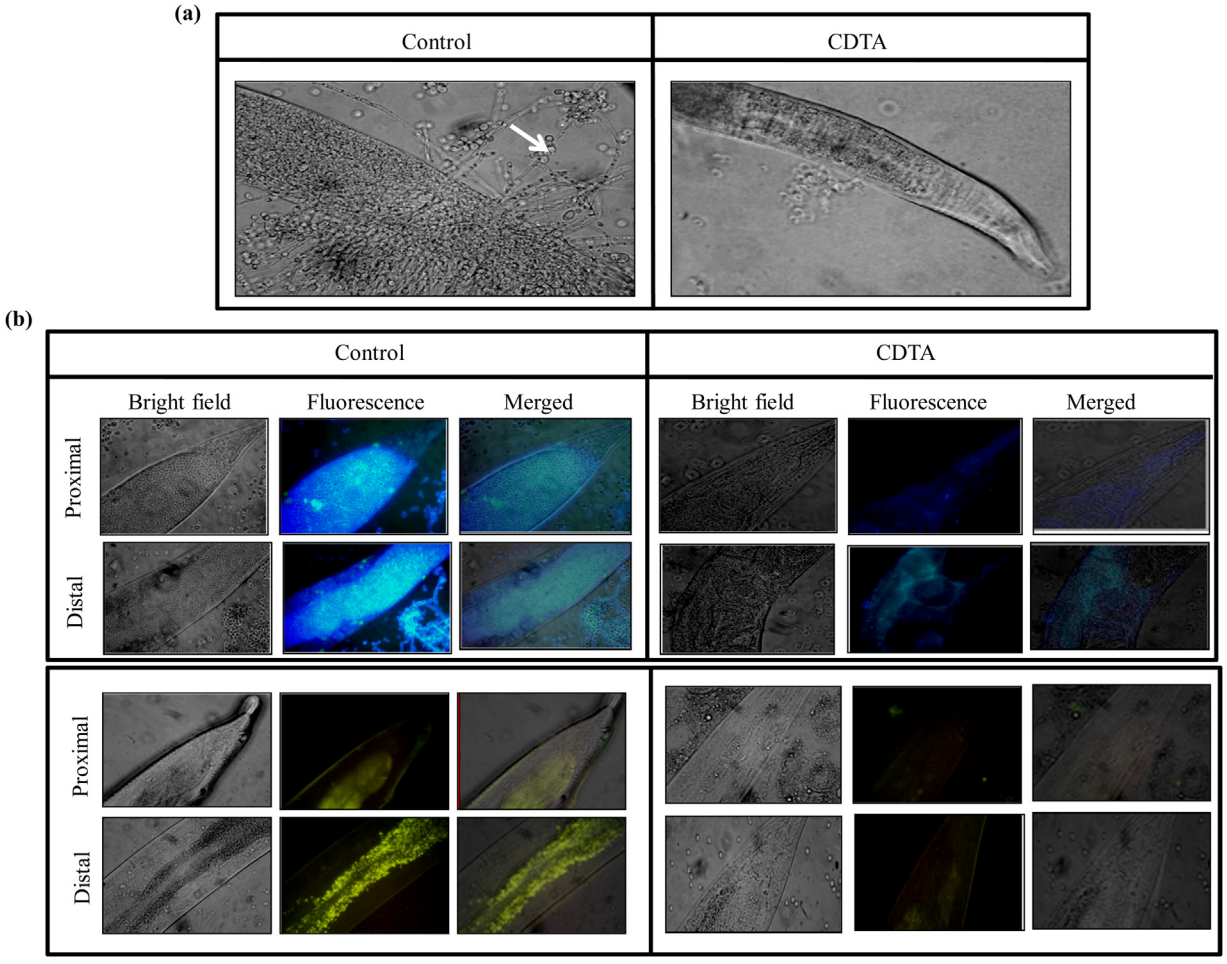

Fig. 10. Hyphal formation and persistence of *Candida albicans* SC5314 in *Caenorhabditis elegans*. (a) Nematodes infected with *C. albicans* SC5314 showed hyphal formation, which was absent in the Mg-deprived condition (25 μg/mL). (b) Calcofluor white staining and Act1p-GFP visualisation of both regions of the nematodes' intestine showing less infection with Mg deprivation.

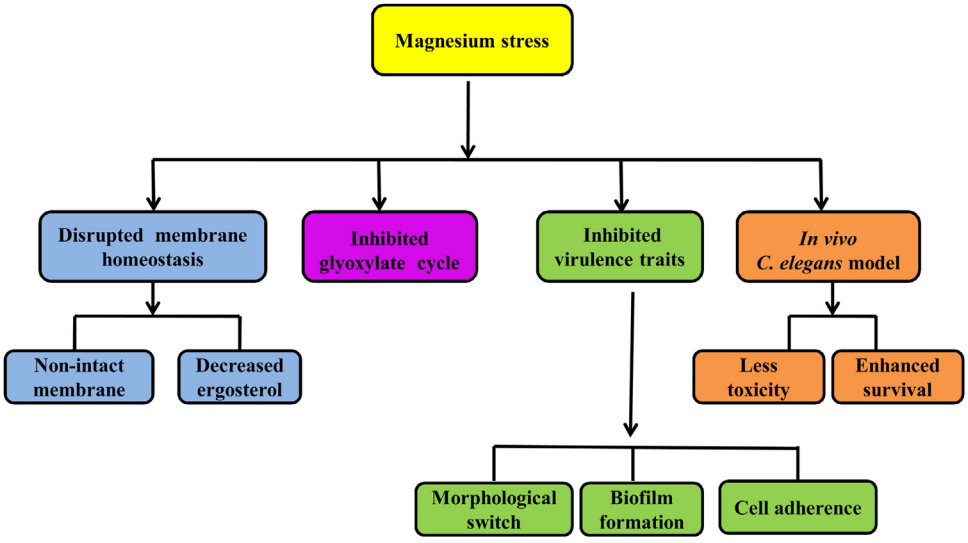

Fig. 11. Model depicting affected cellular circuitry of *Candida albicans* under magnesium stress.

infection in *C. elegans* resulted in no survival in non-treated controls, whereas 20% of worms survived even after 8 days in the presence of Mg deprivation (Fig. 9b).

3.9. Magnesium deprivation reduces hyphal formation and persistence of C. albicans SC5314 in C. elegans

The nematode model study was further extended to explore the ability of *Candida* cells to invade and persist in tissues. First, it was confirmed whether the Mg-deprived condition diminishes hyphal formation of *C. albicans* SC5314 in *C. elegans*, as functional yeast-to-hyphal transition is crucial for invasion of tissues to cause infection. No hyphal formation was observed under Mg deprivation (Fig. 10a). Next, the persistence of *C. albicans* SC5314 in the intestine of *C .elegans* was studied [13]. This was achieved by CFW where on the second day blue-coloured *C. albicans* SC5314 were clearly visible in the proximal and distal intestine of untreated *C. elegans* that were absent in CDTA-treated worms (Fig. 10b). In addition, the constitutively expressed Act1p-GFP strain [20] of *C. albicans* SC5314 was fed to *C. elegans* and worms were monitored for *C. albicans* persistence in the intestine. The presence of *C. albicans* SC5314 was clear from the green fluorescence both in the proximal as well as the distal intestine regions in the untreated control that was again absent in CDTA-treated worms (Fig. 10b).

4. Discussion

The duality of *C. albicans* SC5314 as a human commensal and pathogenic micro-organism exposes it to differences in nutrient accessibility that are associated with diverse environments within the host [21]. Metals play an essential role in all organic systems, where they are incorporated into metalloproteins including transcription factors, storage proteins and enzymes. Thus, a better understanding of micronutrient availability in *C. albicans* could be a novel approach to circumvent multidrug resistance. In a recent study, BPTI inhibited the growth of *C. albicans* by directly targeting Alr1p, a Mg transporter, to block magnesium uptake resulting in growth arrest [4]. Similarly, the broad-spectrum chelator DTPA increased susceptibility to echinocandins via chelation of magnesium only [5]. The present study was therefore designed to elucidate the effect of Mg deprivation on antifungal drug susceptibilities with possible mechanistic insights.

This study demonstrated that Mg chelation improves the antifungal activity of membrane-targeting drugs (Fig. 1). This is in contrast to an earlier study which showed that iron deprivation leads to enhanced susceptibility not only to azoles but also to other classes of antifungals [22], reinforcing the hypothesis that Mg has a specific effect on the cell membrane. Furthermore, we revealed the indispensability of Mg for the functionality of efflux pumps belonging to the ABC transporter superfamily (Fig. 2), which are a major cause of multidrug resistance in *C. albicans* [23,24]. The *C. albicans* cell membrane is a crucial interface in the host–pathogen interaction that mediates a variety of functions, including sensing and signalling to the external environment [25]. The observed enhanced susceptibility to membrane-targeting drugs and inhibition of efflux pump activity encouraged us to examine the membrane more closely. It was observed that the level of ergosterol, which is the main target of membrane-targeting drugs, was reduced under Mg deprivation (Fig. 3). The calcineurin pathway is known to be involved in cell persistence under a variety of cellular stresses (alkaline pH stress, ionic stress, membrane stress) [26]. The calcineurin signalling pathway is a key intermediary of stress responses in *C. albicans* SC5314 and has potential as a therapeutic target. Taking clue from the disrupted membrane homeostasis, we analysed any connection with the calcineurin signalling pathway. It was observed that Mg depletion causes phenotypic susceptibility under all of the tested stress conditions that require a functional calcineurin signalling response (Fig. 4).

The glyoxylate cycle is an alternate to the tricarboxylic acid cycle that provides the route to CO_2-producing steps to preserve carbon when low-carbon conditions prevail. This pathway does not exist in the mammalian host, making it a unique drug target [27,28]. Thus, this metabolic pathway in *C. albicans* SC5314, which allows *C. albicans* SC5314 to live in nutrient-inadequate host niches with its key enzymes (Icl1p and Mls1p), has been predicted as a potential antifungal target to treat candidiasis [29]. Interestingly, we found that the glyoxylate cycle is compromised in the presence of Mg deprivation (Fig. 5).

The morphological switch flanked by yeast and hyphal morphology is a significant virulence factor in *C. albicans* [28]. Similarly, biofilm formation is another virulence attribute of *C. albicans* SC5314 that confers pathogenicity. Biofilms are highly antibiotic-resistant and are therefore significant in clinical infections [30,31]. Interestingly, we found both inhibition of yeast-to-hyphae transition (Fig. 7) and biofilm formation (Fig. 8) of *C. albicans* SC5314 under Mg-deprived condition. Repressed biofilm formation further guided us to study cell adherence, which is the primary step in biofilm formation [32]. Cell adherence of *C. albicans* was reduced both on buccal epithelial cells and a polystyrene surface in the presence of Mg deprivation (Fig. 8b). Interestingly, this observation differed from an earlier study where, despite iron deprivation affecting yeast-to-hyphal transition, it did not affect biofilm formation [22] suggesting that each metal has its own defined role. Finally, in vivo studies using the nematode *C. elegans* were conducted. The survival rate of *C. elegans* was increased by inhibiting the growth of *C. albicans* SC5314 (Fig. 9). This result was also confirmed by increased intestinal persistence of *C. albicans* under Mg-deprived condition (Fig. 10).

5. Conclusion

The data presented here clearly show the effect of Mg deprivation on *C. albicans* SC5314 cellular circuitry (Fig. 11). Considering the growing prominence that metals also have a tremendous impact on *C. albicans* SC5314 virulence and drug resistance, dissecting the mechanisms that govern Mg homeostasis in *C. albicans* SC5314 may hold great promise for revealing new therapeutic strategies for life-threatening fungal diseases.

Acknowledgments

The authors are grateful to Joseph Heitman (*Candida albicans* SC5314 calcineurin mutants), Alistair Brown (Act1p-GFP), Joachim Morschhäuser (matched pair of clinical azole-susceptible and -resistant isolates Gu4 and Gu5), Rajendra Prasad (AD-CDR1 and AD-MDR1) and Michael Lorenz (*ICL1* mutant) for generous gifts. The authors also thank Anindya Ghosh for providing the wild-type *Caenorhabditis elegans* N2 and *Escherichia coli* OP50 strains.

Funding

None.

Competing interests

None declared.

Ethical approval

Not required.

Appendix A. Supplementary data

Supplementary data associated with this article can be found, in the online version, at https://doi.org/10.1016/j.jgar.2019.01.011.

References

[1] Singh S, Fatima Z, Hameed S. Predisposing factors endorsing *Candida* infections. Infez Med 2015;23:211–23.
[2] Lim PH, Pisat NP, Gadhia N, Pandey A, Donovan FX, Stein L, et al. Regulation of Alr1 Mg transporter activity by intracellular magnesium. PLoS One 2011;6: e20896.
[3] de Baaij JH, Hoenderop JG, Bindels RJ. Magnesium in man: implications for health and disease. Physiol Rev 2015;95:1–46.
[4] Bleackley MR, Hayes BM, Parisi K, Saiyed T, Traven A, Potter ID, et al. Bovine pancreatic trypsin inhibitor is a new antifungal peptide that inhibits cellular magnesium uptake. Mol Microbiol 2014;92:1188–97.
[5] Polvi EJ, Averette AF, Lee SC, Kim T, Bahn YS, Veri AO, et al. Metal chelation as a powerful strategy to probe cellular circuitry governing fungal drug resistance and morphogenesis. PLoS Genet 2016;12:e1006350.
[6] Cruz MC, Goldstein AL, Blankenship JR, Del Poeta M, Davis D, Cardenas ME, et al. Calcineurin is essential for survival during membrane stress in *Candida albicans*. EMBO J 2002;21:546–59.
[7] Clinical and Laboratory Standards Institute. Reference method for broth dilution antifungal susceptibility testing of yeasts; approved standard—third edition. Document M27-A3. Wayne, PA: CLSI; 2008.
[8] Singh S, Fatima Z, Hameed S. Insights into the mode of action of anticandidal herbal monoterpenoid geraniol reveal disruption of multiple MDR mechanisms and virulence attributes in *Candida albicans*. Arch Microbiol 2016;198:459–72.
[9] Ansari MA, Fatima Z, Hameed S. Mechanistic insights into the mode of action of anticandidal sesamol. Microb Pathog 2016;98:140–8.
[10] Singh S, Fatima Z, Ahmad K, Hameed S. Fungicidal action of geraniol against *Candida albicans* is potentiated by abrogated CaCdr1p drug efflux and fluconazole synergism. PLoS One 2018;13:e0203079.
[11] Ansari MA, Fatima Z, Hameed S. Anticandidal effect and mechanisms of monoterpenoid, perillyl alcohol against *Candida albicans*. PLoS One 2016;11: e0162465.
[12] Ansari MA, Fatima Z, Hameed S. Cellular energy status is indispensable for perillyl alcohol mediated abrogated membrane transport in *Candida albicans*. ADMET DMPK 2017;5:126–34.
[13] Ansari MA, Fatima Z, Ahmad K, Hameed S. Monoterpenoid perillyl alcohol impairs metabolic flexibility of *Candida albicans* by inhibiting glyoxylate cycle. Biochem Biophys Res Commun 2018;495:560–6.
[14] Zhao LX, Li DD, Hu DD, Hu GH, Yan L, Wang Y, et al. Effect of tetrandrine against *Candida albicans* biofilms. PLoS One 2013;8:e79671.
[15] Franz R, Kelly SL, Lamb DC, Kelly DE, Ruhnke M, Morschhäuser J. Multiple molecular mechanisms contribute to a stepwise development of fluconazole resistance in clinical *Candida albicans* strains. Antimicrob Agents Chemother 1998;42:3065–72.
[16] Shukla S, Saini P, Smriti Jha S, Ambudkar SV, Prasad R. Functional characterization of *Candida albicans* ABC transporter Cdr1p. Eukaryot Cell 2003;2:1361–75.
[17] Pasrija R, Banerjee D, Prasad R. Structure and function analysis of CaMdr1p, a major facilitator superfamily antifungal efflux transporter protein of *Candida albicans*: identification of amino acid residues critical for drug/H^+ transport. Eukaryot Cell 2007;6:443–53.
[18] Blankenship JR, Heitman J. Calcineurin is required for *Candida albicans* to survive calcium stress in serum. Infect Immun 2005;73:5767–74.
[19] Ramirez MA, Lorenz MC. Mutations in alternative carbon utilization pathways in *Candida albicans* attenuate virulence and confer pleiotropic phenotypes. Eukaryot Cell 2007;6:280–90.
[20] Murad AM, Lee PR, Broadbent ID, Barelle CJ, Brown AJ. Clp10, an efficient and convenient integrating vector for *Candida albicans*. Yeast 2000;16:325–7.
[21] Pérez JC, Kumamoto CA, Johnson AD. *Candida albicans* commensalism and pathogenicity are intertwined traits directed by a tightly knit transcriptional regulatory circuit. PLoS Biol 2013;11:e1001510.
[22] Hameed S, Dhamgaye S, Singh A, Goswami SK, Prasad R. Calcineurin signaling and membrane lipid homeostasis regulates iron mediated multidrug resistance mechanisms in *Candida albicans*. PLoS One 2011;6:e18684.
[23] Prasad R, Banerjee A, Khandelwal NK, Dhamgaye S. The ABCs of *Candida albicans* multidrug transporter Cdr1. Eukaryot Cell 2015;14:1154–64.
[24] Prasad R, Rawal MK, Shah AH. *Candida* efflux ATPases and antiporters in clinical drug resistance. Adv Exp Med Biol 2016;892:351–76.
[25] Cabezón V, Llama-Palacios A, Nombela C, Monteoliva L, Gil C. Analysis of *Candida albicans* plasma membrane proteome. Proteomics 2009;9:4770–86.
[26] Juvvadi PR, Lamoth F, Steinbach WJ. Calcineurin as a multifunctional regulator: unraveling novel functions in fungal stress responses, hyphal growth, drug resistance, and pathogenesis. Fungal Biol Rev 2014;28:56–69.
[27] Lorenz MC, Fink GR. Life and death in a macrophage: role of the glyoxylate cycle in virulence. Eukaryot Cell 2002;1:657–62.
[28] Dunn MF, Ramírez-Trujillo JA, Hernández-Lucas I. Major roles of isocitrate lyase and malate synthase in bacterial and fungal pathogenesis. Microbiology 2009;155:3166–75.
[29] Cheah HL, Lim V, Sandai D. Inhibitors of the glyoxylate cycle enzyme ICL1 in *Candida albicans* for potential use as antifungal agents. PLoS One 2014;4: e95951.
[30] Hameed S, Prasad T, Banerjee D, Chandra A, Mukhopadhyay CK, Goswami SK, et al. Iron deprivation induces EFG1-mediated hyphal development in *Candida albicans* without affecting biofilm formation. FEMS Yeast Res 2008;8:744–55.
[31] Ramage G, Saville SP, Thomas DP, López-Ribot JL. *Candida* biofilms: an update. Eukaryot Cell 2005;4:633–8.
[32] Breger J, Fuchs BB, Aperis G, Moy TI, Ausubel FM, Mylonakis E. Antifungal chemical compounds identified using a *C. elegans* pathogenicity assay. PLoS Pathog 2007;3:e18.